

# Gas-phase electronic spectra of $C_6NH_2$ and $C_8NH_2$

A.E. Boguslavskiy, H. Ding, J.P. Maier\*

*Department of Chemistry, University of Basel, Klingelbergstrasse 80, CH-4056 Basel, Switzerland*

Received 13 October 2005; received in revised form 10 December 2005; accepted 12 December 2005

Available online 24 January 2006

## Abstract

The electronic spectra of  $C_6NH_2$  and  $C_8NH_2$  have been detected in the gas phase in the 16700–22000  $cm^{-1}$  range by a mass selective resonant two-color two-photon ionization technique coupled to a laser ablation source. Several possible structural motifs are discussed. The production suggests to be amino radical addition to a linear carbon skeleton ( $C_6NH_2$ ). Calculations indicate that a structure with hydrogens and nitrogen on opposite ends of the molecule ( $H_2C_6N$ ) lies 2.8 eV lower in energy. The absence of  $\sim 20\text{ cm}^{-1}$  spaced rotational K-structure indicates the presence of an off-axis carbon or nitrogen atom, but not hydrogen alone.

© 2006 Elsevier B.V. All rights reserved.

**Keywords:** Optical spectroscopy; Nitrogen containing hydrocarbons; Laser ablation; Electronic transitions

## 1. Introduction

Approximately one quarter of the interstellar and circumstellar molecules detected to date contain nitrogen. The majority of these species have only carbon and hydrogen as additional elements. It is also striking that the longest of these nitrogen containing compounds are cyanopolynes [1]: a carbon skeleton capped by H and N atoms at opposite ends. Such an abundance invokes interest to the mechanism of their formation. As several amino-containing molecules are also detected in space, the study of  $C_nNH_2$  moieties becomes of interest. Spectroscopic characterization of such molecules is desirable also for their identification in plasma and combustion reactions.

The conventional way to produce nitrogen capped carbon species is by applying an electrical discharge through a mixture of acetylene or diacetylene, to provide building blocks for the chains, with cyanoacetylene [2–4], cyanogen [3,5], dicyanogen [6], or even  $N_2$  [2,7] in rare gases. This approach is not thought to be suitable for the amino-capping: introduction of ammonia or similar precursors precludes creation of long chains by blocking the growing end of the “assembly line”. Alternatively, one could

first grow a carbon skeleton and then expose the species to a reactant like  $NH_3$ . Thus, a source that utilizes laser ablation of graphite has been adopted.

The products from graphite vaporization in reactive atmospheres have been studied mainly mass-spectroscopically. In one study it was shown that the small even carbon species are as reactive as the odd-numbered ones, but become resistant to reactions with NO,  $H_2$ , CO,  $SO_2$ ,  $O_2$ , and  $NH_3$  in the 40–80 atoms range [8]. In the study of the carbon molecules comprising 6–30 atoms in the presence of  $H_2$ ,  $H_2O$ , and  $N_2$ , the most abundant products were  $C_{2n}H_2$  (and  $C_{2n}N_2$  for  $N_2$ ) implying linear skeleton structures [9]. At high hydrogen concentrations the peaks  $C_{2n}H_{m=6,8,\dots}$  became apparent, confirming the presence of also non-linear carbon moieties in the plasma. The abundance of the  $C_{2n}H_2$  products is attributed to their inert nature. In the recent study of ablated graphite in  $H_2$  and  $D_2$  gases, it was shown that at short delays after the laser pulse, the amount of other derivatives ( $C_nH_m$ ) is significant [10]. Although mass-spectroscopic techniques give an indication as to the structure of the most abundant products, proof can be provided by spectroscopy. Recently, the cyclic and linear isomers of  $C_{18}$  and  $C_{22}$  formed by laser vaporization could be distinguished by addition of hydrogen and the subsequent identification of the electronic transition of the formed  $HC_{2n}H$  chains [11].

In this contribution the gas phase electronic spectra of  $C_6NH_2$  and  $C_8NH_2$  created in an ammonia seeded graphite ablation are presented. Products were detected via a resonance-

\* Corresponding author. Tel.: +41 61 267 3826; fax: +41 61 267 3855.

E-mail addresses: J.P.Maier@unibas.ch (J.P. Maier),  
A.Boguslav@unibas.ch (A.E. Boguslavskiy)

enhanced multiphoton ionization (REMPI) scheme under supersonic molecular-beam conditions. Several possible isomers are discussed in relation to the plasma chemistry. Electronic and vibrational information is considered and the implications discussed.

## 2. Experiment

The apparatus consisted of a molecular beam combined with a linear time-of-flight (TOF) mass analyzer. The source relied on laser vaporization of graphite coupled to a pulsed valve. The rod was rotated and translated so that a fresh surface was continuously exposed to the laser (25 mJ/5 ns pulse of 532 nm Nd:YAG, focused to 0.3 mm) which was fired to coincide with the buffer gas flow over the target area. Vaporized carbon was swept through a 15 mm long and 3 mm diameter tube with ammonia (10%) seeded neon at 5–10 bar and expanded into a vacuum chamber. The species produced passed through a skimmer into a differentially pumped region where ions were removed by a perpendicular electrical field before entering the TOF. The neutral molecules were then ionized by 7.9 eV photons of a F<sub>2</sub> laser. The ionization process is more efficient when the tunable laser is resonant with a dipole-allowed electronic transition. Ions were extracted and accelerated towards a dual micro-channel plate detector. Photons in the 440–620 nm range were delivered by an OPO system ( $\approx 0.25 \text{ cm}^{-1}$  bandwidth). The latter was anti-collinear to the molecular beam, while the ionization laser was perpendicular, allowing for maximum overlap. Variation of the mass-peak area as function of the laser wavelength gives the REMPI spectrum of the molecule. Separation of the ions in the drift tube after resonant excitation enables a large number of masses to be monitored simultaneously.

## 3. Results and discussion

### 3.1. Observations

Fig. 1 shows the measured electronic excitation spectra of C<sub>6</sub>NH<sub>2</sub> (a) and C<sub>8</sub>NH<sub>2</sub> (b) in the 17000–22000 cm<sup>−1</sup> range. The maxima of the observed vibronic bands are given in Tables 1 and 2. The molecular formulae of the carriers were determined from the mass-to-charge ratio ( $m/z$ ) of the ions detected. Isotopic labelled precursor was utilized to distinguish moieties like NC<sub>5</sub>N and C<sub>7</sub>H<sub>4</sub> from C<sub>6</sub>NH<sub>2</sub>, which all have the same  $m/z=88$ . The optical spectrum moves to the  $m/z=90$  channel on deuteration, confirming the presence of two hydrogens.

The spectrum of C<sub>6</sub>NH<sub>2</sub> appears to have its origin at 19691 cm<sup>−1</sup>. No other absorptions were observed at lower energy down to 16200 cm<sup>−1</sup>. While the majority of the spectral lines are  $\sim 5 \text{ cm}^{-1}$  wide, a few peaks at the blue end are noticeably broader ( $\sim 30 \text{ cm}^{-1}$ ). Predissociation does not appear to be involved because no resonance peaks by smaller masses (down to  $m/z=40$ ) were observed at the same wavelength. The broadened features could have been attributed to a transition to the next electronic state, which would be expected to have a shorter lifetime due to efficient internal conversion to the underlying A-state. However, the analysis of two spectra

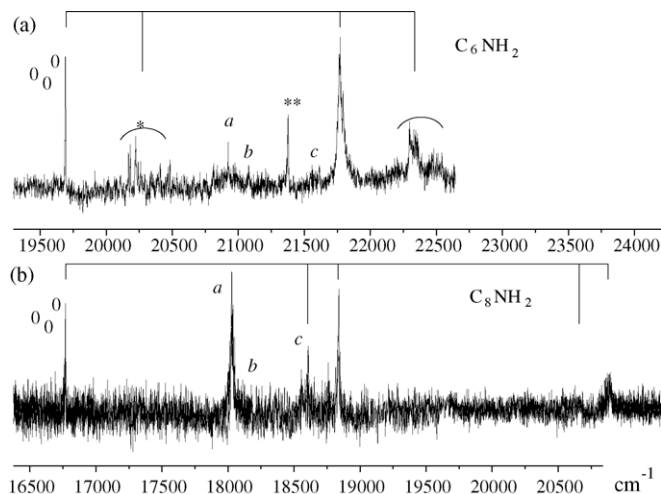


Fig. 1. Gas phase electronic spectra of (a) C<sub>6</sub>NH<sub>2</sub> and (b) C<sub>8</sub>NH<sub>2</sub> detected by a resonant two-color two-photon ionization technique under supersonic molecular beam conditions. Both show the excitation of C≡C modes. Laser bandwidth increases from  $\approx 0.2$  to  $0.3 \text{ cm}^{-1}$  at higher energy. Letters refer to the peaks that have counterparts in both spectra, and stars—for those that do not.

traces the corresponding features for a C<sub>8</sub>NH<sub>2</sub> molecule involving  $\sim 2100 \text{ cm}^{-1}$  C≡C-stretch progression. Thus, peak 19(20) is assigned to the vibronic transition  $\nu_{(C\equiv C)_0^1}$  of C<sub>6</sub>NH<sub>2</sub>, and peaks 6, 9 of C<sub>8</sub>NH<sub>2</sub> to  $\nu_{(C\equiv C)_0^1}$  and  $\nu_{(C=C)_0^2}$ . Additional bands to higher energy then appear to be due to combinations of this stretch with other lower frequency modes. There are also other similarities between the two spectra: the bands *a*, *b*, *c* in Fig. 1 seen to be common to C<sub>6</sub>NH<sub>2</sub> and C<sub>8</sub>NH<sub>2</sub>. Different width and pattern of the vibronic bands in the two spectra suggests

Table 1

Maxima of the vibronic bands observed in the electronic spectrum of C<sub>6</sub>NH<sub>2</sub>

Peak	$\nu \text{ (cm}^{-1}\text{)}$	$\Delta\nu \text{ (cm}^{-1}\text{)}$	Assignment
1	19691(1)	0	$0_0^0$
2	19845(2)	154	
3	19915(2)	224	
4	20106(3)	415	
5	20169(1)	478	$\nu_*$
6	20183(1)	492	
7	20224(2)	533	
8	20242(1)	551	
9	20261(1)	571	
10	20292(1)	601	
11	20340(1)	649	
12	20409(1)	718	
13	20484(2)	793	
14	20922(2)	1231	$\nu_a$
15	21078(2)	1387	$\nu_b$
16	21375(2)	1684	$\nu_{**}$
17	21547(3)	1856	$\nu_c$
18	21614(2)	1923	
19	21767(10)	2076	$(\nu_{C\equiv C})_0^1$
20	21795(2)	2104	
21	21905(10)	2214	$(\nu_{C\equiv C})_0^1 + \nu_*$
22	22297(10)	2606	
23	22341(15)	2650	
24	22469(5)	2778	
25	22542(5)	2851	

Table 2  
Maxima of the vibronic bands observed in the electronic spectrum of  $C_8NH_2$

Peak	$\nu$ ( $cm^{-1}$ )	$\Delta\nu$ ( $cm^{-1}$ )	Assignment
1	16769(1)	0	$0_0^0$
2	18028(2)	1259	$\nu_a$
3	18176(2)	1407	$\nu_b$
4	18558(4)	1789	$\nu_c$
5	18608(3)	1839	
6	18840(4)	2071	$(\nu_{C\equiv C})_0^1$
7	19659(15)	2890	
8	20665(20)	3896	$(\nu_{C\equiv C})_0^1 + \nu_c$
9	20893(5)	4124	$(\nu_{C\equiv C})_0^2$
10	21612(15)	4843	

coupling of a “bright state” with a “dark state”. This depends on their proximity, which would be different among these two molecules.

### 3.2. Structural considerations

In the absence of resolved rotational structure other spectroscopic and theoretical information has to be used to infer the likely structure of the species. The mass spectra provide information on the most abundant products in the plasma and gives  $C_nH$ ,  $C_n$ ,  $C_nH_2$ ,  $C_nNH_4$ ,  $C_nH_3$ ,  $C_nH_4$ . No prominent amounts of N-, NH-, or  $NH_2$ -capped species were detected suggesting that the fragmentation  $H_3N \rightarrow H_2N^\bullet + H^\bullet$  occurs without further dissociation of amidogen. Hydrogen radical makes a stronger bond with hydrocarbons than the amino radical  $H_2N^\bullet$  (see Table 2 in [12]) and is lighter and more agile. So it is expected that an H atom will react more effectively with the growing carbon chains than  $H_2N^\bullet$ . This explains the prevalence of the hydrogen capped chains in the mass-spectrum.

The apparent abundance of long chains in graphite ablation in presence of ammonia suggests that the major part of the reactions with it takes place after the growth of a carbon skeleton. Plasma at the point of the laser spot is constricted at the high buffer gas pressure and clustering reactions are rapid in the plume of carbon vapor compared with the diffusion speed [9]. Thus, the dominant products are expected to be one or both end-capped carbon moieties rather than those with a nitrogen atom inserted into the chain. This would also be in agreement with the spectro-

scopic detection of  $C_6NH_2$  and  $C_8NH_2$ , belonging to the same family.

Several possible structural isomers of  $C_6NH_2$  were calculated at the DFT-B3LYP/6-31G(2df) level and the results, along with their symmetry group and relative energy, are depicted in Fig. 2. The three simplest candidates (isomers 1–3) are considered first. Isomer 1 complies with the above considerations in the most straightforward way, arising via attachment of  $H_2N^\bullet$  to a bare carbon chain in the plasma region. An unsaturated carbon chain pulls electronic density away from the nitrogen atom, forcing the molecule to flatten. The reaction mechanism for production of isomer 2 is less evident, even though it lies 2.81 eV lower in the energy than isomer 1. The formation could involve multiple collisions, which take place in the source, causing sequential H-atom additions to the opposing end of chain. Alternatively, hydrogens from one end of carbon skeleton to the other have to migrate. However, this barrier may not be crossed because of fast adiabatic cooling in the supersonic expansion. The latter is known to be efficient, sometimes freezing the reaction products before they anneal to the lowest energy conformation. An example is the detection of a  $C_7H_3$  isomer lying 2.1 eV above the most stable form [13]. Isomer 3 ( $C_s$ ) of  $C_6NH_2$  is an intermediate form between the first two.

The absence of a clear K-structure (the rotational A constants for isomers 1 and 2 are  $\approx 10\text{ cm}^{-1}$ , for 3  $\approx 25\text{ cm}^{-1}$ ) in the optical spectra restricts all measured vibronic transitions to be of A-type. As the presence of only this type of transitions seems unlikely, this leads to the consideration of structures with off-axis heavy atoms (i.e., non-hydrogen) to decrease the A-constant. If there would be just H-atoms off-axis, the K-structure would be clearly resolved (as has been observed in molecules such as  $H_2CCC$  [14]). Structures 4–8 comply with this requirement and possess an acetylenic triple bond. They also easily tolerate the addition of two carbon atoms.  $(4n + 3)$ -membered rings become stabilized upon removing the excess electron from the  $\pi$ -orbital system, be it done by ionization, or forming a  $\sigma$  lone pair like in cyclopropenylidene, or delocalizing it on an adjacent unsaturated carbon chain. Different permutations of end-CH and N generate the structures 3–6. The microwave observations of the ring-chains  $C_nH_2$ ,  $n = 5, 7, 9$  [15–17] and  $HC_nN$ ,  $n = 4, 6$  [18] further point to the existence of corresponding  $C_nNH_2$  species.

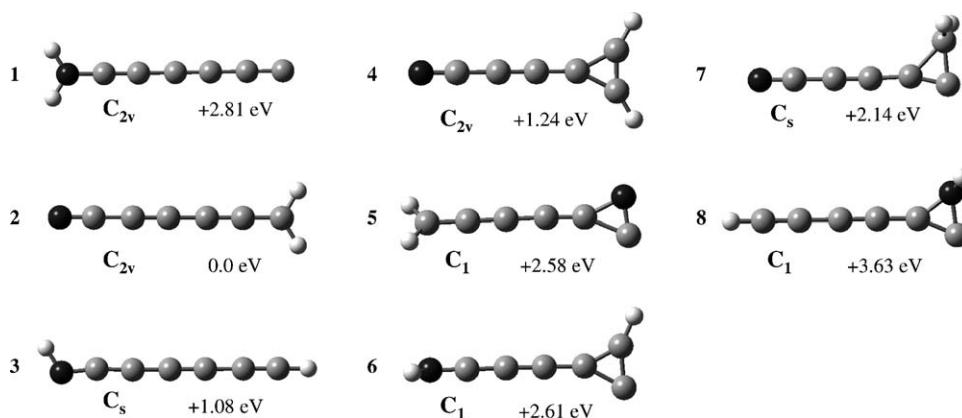


Fig. 2. Possible structural isomers of  $C_6NH_2$  and the relative stabilities calculated at the DFT-B3LYP/6-31G(2df) level.

In isomers 7 and 8 the conjugated system will behave spectroscopically like in a linear chain. One would expect these  $C_6NH_2$  molecules to exhibit an electronic spectrum analogous to linear  $C_6H$ , which was first measured in absorption in a neon matrix [19]. The  $C_6H$  radical absorbs in the same region as  $C_6NH_2$  and exhibits similarities in its pattern of vibronic transitions. One can compare the acetylenic stretch vibrations  $3_0^1$  ( $1638\text{ cm}^{-1}$ ) and  $5_0^1$  ( $2076\text{ cm}^{-1}$ ) of  $C_6H$  with  $\nu_{\star\star}$  ( $1684\text{ cm}^{-1}$ ) and  $\nu_{(C\equiv C)_0^1}$  ( $2076\text{ cm}^{-1}$ ) of  $C_6NH_2$ . The shift of the  $C_6NH_2$  origin by  $\sim 800\text{ cm}^{-1}$  to the blue of that of  $C_6H$  is probably mostly due to the  $CH\rightarrow N$  substitution effects, which for linear chains are normally of the order of a thousand wavenumbers. Besides, the shift of the absorption origin upon adding two carbons  $C_6NH_2$  to  $C_8NH_2$  ( $2922\text{ cm}^{-1}$ ) is similar to that ( $3016\text{ cm}^{-1}$ ) from  $C_6H$  [20] to  $C_8H$  [21]. This shift is a normal behavior of conjugated carbon chains belonging to a homologous series.

The spectra of the “isoelectronic” series  $C_9H_3$ ,  $C_{11}H_3$ ,  $C_{13}H_3$  should be mentioned. These species were found to absorb all in the same part of the visible range [22], exhibiting remarkably similar vibrational structure and low ionization potentials ( $<6.4\text{ eV}$ ). However,  $C_6NH_2$  and  $C_8NH_2$  must possess a different structure to their isoelectronic  $C_mH_3$  analogs since they have an ionization potential  $>7.9\text{ eV}$  and the origin band position shifts about  $3000\text{ cm}^{-1}$  to the red upon adding two carbon atoms.

#### 4. Concluding remarks

The electronic spectra of two nitrogen containing hydrocarbon radicals resulting from graphite ablation in the presence of  $NH_3/Ne$  are reported. The mass-spectra indicate  $C_6NH_2$  and  $C_8NH_2$  for their composition. While the absence of rotational structure precludes a definitive assignment of their geometry, the vibronic pattern in the electronic spectra is used as an indication of this. Candidate structures must possess a conjugated carbon chain skeleton to be consistent with the trend in the excitation energy within a homologous series. Both species have to have an off-axis carbon or nitrogen atom in a three-membered ring attached to a conjugated carbon chain and one or two hydrogens.

Although several isomers are likely to be present in the plasma, as has been shown by microwave studies of the related  $C_5H_2$  species [15] where as many as four different conformations were identified, it seems that only one of structures is being picked out by the REMPI technique used. Apart from the existence of potential barriers between different structures and the rapid cooling capability of a supersonic jet expansion, there are specific limitations of the experimental method. Sensitivity on the ionization potential, ionization efficiency with given photon energy of an isomer, and fast intramolecular dynamics in the excited states may prevent the electronic spectra of other isomers

to be measured. The latter criterion rather than the relative abundance or lowest energy is likely the most important factor and is thought to be responsible for the non-detection of other isomers. The fact that these nitrogen containing molecules were detected implies a slow ( $\sim 30\text{ ns}$  for  $C_6NH_2$  and  $\sim 5\text{ ns}$  for  $C_8NH_2$ ) internal conversion from the measured excited state and hence a large energy gap above the ground state. This provides a further means to confirm their structure once good quality ab initio calculations of the excitation energies become available.

#### Acknowledgement

This work has been supported by the Swiss National Science Foundation (project 200020-100019).

#### References

- [1] M.B. Bell, P.A. Feldman, M.J. Travers, M.C. McCarthy, C.A. Gottlieb, P. Thaddeus, *Astrophys. J.* 483 (1997) 61.
- [2] V.D. Gordon, M.C. McCarthy, A.J. Apponi, P. Thaddeus, *Astrophys. J.* 540 (2000) 286.
- [3] O. Vaizert, T. Motylewski, M. Wyss, E. Riaplov, H. Linnartz, J.P. Maier, *J. Chem. Phys.* 114 (2001) 7918.
- [4] M.C. McCarthy, J.-U. Grabow, M.J. Travers, W. Chen, C.A. Gottlieb, P. Thaddeus, *Astrophys. J.* 494 (1998) 231.
- [5] H. Linnartz, O. Vaizert, P. Cias, L. Gruter, J.P. Maier, *Chem. Phys. Lett.* 345 (2001) 89.
- [6] H. Ding, A.E. Boguslavskiy, T.W. Schmidt, J.P. Maier, *Chem. Phys. Lett.* 392 (2004) 225.
- [7] M.C. McCarthy, E.S. Levine, A.J. Apponi, P. Thaddeus, *J. Mol. Spectrosc.* 203 (2000) 75.
- [8] Q.L. Zhang, S.C. O'Brien, J.R. Heath, Y. Liu, R.F. Curl, H.W. Kroto, R.E. Smalley, *J. Phys. Chem.* 90 (1986) 525.
- [9] J.R. Heath, Q. Zhang, S. O'Brien, R.F. Curl, H.W. Kroto, R.E. Smalley, *J. Am. Chem. Soc.* 109 (1987) 359.
- [10] Y. Kato, T. Wakabayashi, T. Momose, *Chem. Phys. Lett.* 386 (2004) 279.
- [11] A.E. Boguslavskiy, H. Ding, J.P. Maier, *J. Chem. Phys.* 123 (2005) 034305.
- [12] S.J. Blanksby, G.B. Ellison, *Acc. Chem. Res.* 36 (2003) 255.
- [13] H. Ding, T. Pino, F. Guethe, J.P. Maier, *J. Am. Chem. Soc.* 125 (2003) 14626.
- [14] A. Chirokolava, P. Birza, M. Araki, P. Kolek, J.P. Maier, *J. Mol. Spectrosc.* 229 (2005) 276.
- [15] C.A. Gottlieb, M.C. McCarthy, V.D. Gordon, J.M. Chakan, A.J. Apponi, P. Thaddeus, *Astrophys. J.* 509 (1998) 141.
- [16] M.C. McCarthy, M.J. Travers, C.A. Gottlieb, P. Thaddeus, *Astrophys. J.* 483 (1997) L139.
- [17] M.C. McCarthy, M.J. Travers, W. Chen, C.A. Gottlieb, P. Thaddeus, *Astrophys. J.* 498 (1998) 89.
- [18] M.C. McCarthy, J.U. Grabow, M.J. Travers, W. Chen, C.A. Gottlieb, P. Thaddeus, *Astrophys. J.* 513 (1999) 305.
- [19] P. Freivogel, J. Fulara, M. Jakobi, D. Forney, J.P. Maier, *J. Chem. Phys.* 103 (1995) 54.
- [20] M. Kotterer, J.P. Maier, *Chem. Phys. Lett.* 266 (1997) 342.
- [21] H. Linnartz, T. Motylewski, J.P. Maier, *J. Chem. Phys.* 109 (1998) 3819.
- [22] T.W. Schmidt, A.E. Boguslavskiy, T. Pino, H. Ding, J.P. Maier, *Int. J. Mass. Spectrom.* 228 (2003) 647.